Structure and the Electronic Properties of a Jahn–Teller Distorted Tetrahedral Nickel(II) Complex with Sulfur Ligands§

Andreas Wilk,†,‡ Michael A. Hitchman,*,† Werner Massa,‡ and Dirk Reinen*,‡

Fachbereich Chemie und Zentrum für Materialwissenschaften, Philipps-Universität, D-3550 Marburg, Germany, and Chemistry Department, University of Tasmania, Box 252C, Hobart, Tasmania 7001, Australia

Received June 12, 1992

The crystal structures of the compounds $[M(NMTP)]_4(BF_4)_2$ (M = Zn^{2+}, Ni^{2+}; NMTP = *N*-methyl-2-thioxopyrrolidine) are reported. Whereas the zinc(II) complex has a nearly regular tetrahedral geometry, the nickel(II) complex is significantly distorted in the manner predicted by the Jahn–Teller theorem, with *trans*-SNiS angles decreasing from the tetrahedral value of 109.5 to 85°. Metal–ligand bonding parameters have been derived from an analysis of the optical spectrum of $[Ni(NMTP)]_4(BF_4)_2$. Jahn–Teller coupling coefficients and the force constant of the vibronically active ϵ mode have been estimated from the experimental data. The influence of the $3d_{z^2}$–4s interaction on these parameters was studied by calculating the variation of the ground-state energy along the ϵ distortion path.

Introduction

Although the Jahn–Teller theorem predicts that a regular tetrahedral stereochemistry is unstable for four-coordinate, high-spin nickel(II) complexes,[1] the tetrachloronickelate(II) ion is observed to adopt an almost undistorted tetrahedral geometry.[2] Initially, it was suggested[3] that this might be because the orbital degeneracy of the $^3T_1$ ground state is removed by spin–orbit coupling, generating a Γ_1 split state as the new ground state. However, this argument is expected to be invalid if the Jahn–Teller coupling dominates the spin–orbit interaction.[4] In contrast the analogous tetrachlorocuprate(II) polyhedron with a $^3T_2$ ground state exhibits significant enlargements of the ClCuCl angles in comparison to 109.5° in a series of compounds,[5] though the spin–orbit coupling constant of Cu^{2+} is greater than that of Ni^{2+}. The causes of this difference in behavior between tetrahedral nickel(II) and copper(II) complexes have been the subject of a detailed study.[4] It is demonstrated that the former exhibits relatively small distortions because the interaction of the $_a{}^3T_1$ ground state with an excited state of the same symmetry $_b{}^3T_1$ reduces the electronic Jahn–Teller coupling considerably. The strength of this interaction is lowered, if Δ increases and B decreases.

The degeneracy of a T ground state can be lifted by a vibronic coupling with tetrahedral modes of ϵ and τ_2 ($2x$) symmetry. Theoretical considerations and experimental results clearly show that the $T \otimes \epsilon$ interactions dominate. Thus, tetrahedral copper(II) and nickel(II) complexes should both undergo angular distortions which produce a D_{2d} geometry. For the former metal ion this involves an increase in *trans*-LML angles, while for the latter a decrease is expected. Very probably ligand–ligand repulsions associated with a decrease in the *trans*-LML angles also tend to destabilize the distorted geometry in the case of four-coordinated nickel(II) complexes.

The Jahn–Teller coupling constants of Cu^{2+} and Ni^{2+} in a tetrahedral complex mainly depend upon the σ-bonding strength of the ligands (see below).[4] The above arguments imply that a significant distortion away from a regular tetrahedron should occur when relatively strong and polarizable ligands, which also have the property of significantly reducing the interelectron repulsion parameters of the metal, bond to nickel(II) (though these characteristics should not be so well developed that low-spin, planar complexes form).[4] The choice of polarizable ligands has the additional advantage that the restoring force, which opposes the tendency towards distortion, is rather small. Recent studies[6–10] have shown that various sulfur-donor ligands form distorted tetrahedral nickel(II) complexes, though it is not clear in these cases whether ligand and host lattice strains or the vibronic Jahn–Teller coupling (or even all these factors) generate these distortions. In order to investigate the above factors more fully we have prepared the compound $[Ni(NMTP)_4](BF_4)_2$, where NMTP is the ligand *N*-methyl-2-thioxopyrrolidine.

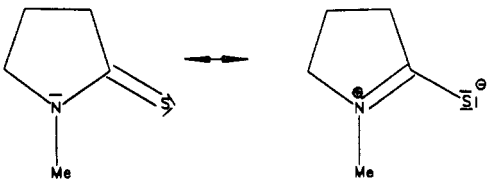

The crystal structure and electronic spectrum of the compound are reported, and in order to properly evaluate the influence of the Jahn–Teller effect upon the stereochemistry, the corresponding zinc(II) and cobalt(II) complexes with spherically symmetric electron clouds have also been studied. The metal–ligand bonding in the nickel and cobalt complexes has been investigated using the angular overlap model (AOM), and the factors influencing vibronic Jahn–Teller interactions in the nickel(II) complex have been analyzed.

* Address correspondence to one of these authors.
† University of Tasmania.
‡ Philipps-Universität.
§ Dedicated to Prof. Dr. R. Hoppe on the occasion of his 70th birthday.

(1) Reinen, D. *Comments Inorg. Chem.* **1983**, *2*, 227.
(2) Pauling, P. *Inorg. Chem.* **1966**, *5*, 1498.
(3) Liehr, A. D.; Ballhausen, C. *J. Ann. Phys. (N.Y.)* **1959**, *6*, 134.
(4) Reinen, D.; Atanasov, M.; Nikolov, G. St.; Steffens, F. *Inorg. Chem.* **1988**, *27*, 1678.
(5) For a recent complation of compounds containing the tetrachlorocuprate ion, see: McDonald, R. G.; Riley, M. J.; Hitchman, M. A. *Inorg. Chem.* **1988**, *27*, 894.
(6) Churchill, M.; Cooke, J.; Fennessey, J. P.; Wormald, J. *Inorg. Chem.* **1971**, *10*, 1031.
(7) Swenson, D.; Baenzinger, N. C.; Coucouvanis, D. *J. Am. Chem. Soc.* **1978**, *100*, 1932.
(8) Yamamura, T.; Miyamae, H.; Katayama, Y.; Sasaki, Y. *Chem. Lett.* **1985**, 268.
(9) Rosenfield, S.; Armstrong, W. H.; Mascharak, P. K. *Inorg. Chem.* **1986**, *25*, 3014.
(10) Kläui, W.; Schmidt, K.; Bockmann, A.; Brauer, D. J.; Wilke, J.; Lueken, H.; Elsenhans, U. *Inorg. Chem.* **1986**, *25*, 4125.

0020-1669/93/1332-2483$04.00/0

Table I. Experimental Data for the Crystal Structure Determinations of $[M(NMTP)_4](BF_4)_2 \cdot solv$ (M = Ni, Zn)

	$Ni(NMTP)_4$-$(BF_4)_2 \cdot 2MeOH$	$Zn(NMTP)_4$-$(BF_4)_2 \cdot DMP$
	Crystal Data	
formula	$C_{22}H_{44}B_2F_8N_4O_2S_4Ni$	$C_{25}H_{48}B_2F_8N_4O_2S_4Zn$
cryst size, mm^3	0.2 × 0.25 × 0.1	0.15 × 0.35 × 0.78
abs μ, cm^{-1}	8.3; no cor	9.7; no cor
space group	$P2_1/n$, $Z = 4$	$C2/c$, $Z = 4$
lattice const		
a, pm	1580.9(5)	1321.3(3)
b, pm	2375.0(9)	2361.7(6)
c, pm	955.3(4)	1322.8(3)
β, deg	90.27(3)	110.94(1)
temp, K	177	223
D_c, g cm^{-3}	1.343	1.385
	Data Collection	
diffractometer	4-circle, CAD4 (Enraf-Nonius)	
radiation	Mo Kα, graphite monochromator	
scan type	ω-scan	
scan width, deg	$(0.9 + 0.35 \tan\theta)$	$(1.5 + 0.3 \tan\theta)$
	and 25% on the left- and right-hand side of a reflcn for bkgd determ	
meas range θ, deg	2–23; $\pm h,+k,+l$	2–25; $\pm h,+k,+l$
tot. no of reflcns	5262	4406
no of reflcns: unique/used $[F_o > 3\sigma(F_o)]$	4925/4175	3355/2565
	Computing	
programs	SHELXTL-plus[14]	
atomic scattering factors	for neutral atoms; $\Delta f'$ and $\Delta f''$ from ref 15	
refinement	full-matrix least squares, $\sum w(F_o - F_c)^2$ minimized, $w = 1/\sigma^2(F)$	
residuals R/R_w	0.083/0.086	0.057/0.047
goodness of fit	4.67	1.89
max. parameter shift/esd	0.003	0.01
$\Delta\rho_{max/min}$, e/Å^3	1.61/–0.78 (at Ni)	0.42/–0.41

Experimental Section

Preparation and Physical Methods. The complexes $[M(NMTP)_4](BF_4)_2 \cdot xL$ [M^{II} = Ni, Co, Zn; L = solvent molecule; see below] were prepared following the procedure of Gritzner et al.[11,12] and, after vigorous drying in a desiccator over phosphorus pentoxide, gave the following analytical results (percent by weight, the data calculated for the solvent-free compounds is given in parentheses). M = Co: C = 34.04 (34.63); H = 5.33 (5.20); N = 7.86 (8.08). M = Ni: C = 33.45 (34.64); H = 5.27 (5.24); N = 7.80 (8.08). M = Zn: C = 34.18 (34.33); H = 4.78 (5.19); N = 7.83 (8.01).

Single crystals suitable for the X-ray investigation were obtained by cooling a 2,2-dimethoxypropane (DMP) solution of the Ni^{2+}-complex to –15 °C. The crystals were picked out of the solution and cooled rapidly because they undergo fast decomposition. Single crystals of the Zn^{2+} complex were obtained by adding an equal volume of methanol to the 2,2-dimethoxypropane solution and cooling to –15 °C. The colorless crystals were used instantly, because they also decompose, leaving opaque white crystals. Single crystals of the Zn^{2+} complex doped with ≈30 mol % Ni^{2+} were formed by dissolving the hydrates in the desired ratio in 2,2-dimethoxypropane, and following the procedure described for the pure Zn^{2+} compounds. The single crystals, used for the structural investigation, contained solvent molecules, which were identified as dimethoxypropane in the case of Zn^{2+} and, most likely, as methanol for the Ni^{2+} complex.

Electronic reflectance spectra were recorded using a Zeiss PMQ II spectrophotometer with a low-temperature attachment, using freshly sintered MgO as a standard. The extent of reflexion was transformed into absorption intensity data log (k/s) (k and s are absorption and scattering coefficients, respectively) using the theory of Kubelka–Munk.

Single crystal electronic spectra were measured on a Cary 17 spectrophotometer using a technique described previously.[13] The crystals were cooled using a Cryodyne Model 21 cryostat fitted with an Oxford Instruments temperature controller and sensor.

Crystal Structure Determinations. Diffraction data were collected on a four-circle diffractometer at low temperatures. The crystallographic data and experimental conditions are summarized in Table I. The lattice constants were refined from a set of 21 (Ni) or 25 (Zn) high-angle reflections. The monoclinic angle is very near to 90° for the Ni^{2+} complex, while in the case of the Zn^{2+} compound, a is nearly equal to c providing us also with the possibility to transform the monoclinic into an orthorhombic unit cell. However, despite the possible orthorhombic metricity in both structures, the Laue symmetry was clearly monoclinic in each case. The structures were solved by direct methods[14] and Fourier techniques.

Table II. Atomic Parameters and Equivalent Isotropic or Isotropic[a] Temperature Factors in $[Ni(NMTP)_4](BF_4)_2 \cdot 2MeOH$. (Hydrogen Atoms Omitted; C/O90–96 = Disordered Methanol Positions;[b] Not Refined)

atom	x	y	z	U_{eq}/U_{iso}
Ni	0.37190(5)	0.21879(4)	0.0859(1)	0.0512(3)
S1	0.3722(1)	0.1995(1)	0.3198(2)	0.0565(7)
S2	0.4681(1)	0.1759(1)	–0.0581(2)	0.0605(7)
S3	0.2724(1)	0.1793(1)	–0.0582(2)	0.0622(7)
S4	0.3711(1)	0.3111(1)	0.1538(2)	0.0573(7)
N1	0.3711(3)	0.1052(3)	0.4660(6)	0.051(2)
N2	0.6356(3)	0.1728(3)	–0.0633(6)	0.058(2)
N3	0.1055(4)	0.1762(3)	–0.0573(8)	0.069(3)
N4	0.3736(4)	0.4073(3)	0.0159(7)	0.062(3)
C11	0.3708(3)	0.1299(3)	0.3435(7)	0.051(3)
C12	0.3686(6)	0.0851(3)	0.2325(9)	0.074(3)
C13	0.3705(7)	0.0297(4)	0.309(1)	0.091(4)
C14	0.3686(5)	0.0440(4)	0.4636(8)	0.068(3)
C15	0.3728(6)	0.1341(4)	0.6000(8)	0.082(4)
C21	0.5668(4)	0.1922(3)	–0.0023(7)	0.050(2)
C22	0.5893(4)	0.2304(3)	0.1133(8)	0.058(3)
C23	0.6853(5)	0.2343(5)	0.108(1)	0.091(4)
C24	0.7148(5)	0.1923(4)	0.003(1)	0.077(4)
C25	0.6381(5)	0.1335(5)	–0.180(1)	0.095(4)
C31	0.1748(4)	0.1950(3)	0.0029(8)	0.057(3)
C32	0.1547(4)	0.2280(4)	0.1303(9)	0.075(3)
C33	0.0576(5)	0.2309(5)	0.131(1)	0.109(5)
C34	0.0282(5)	0.1943(5)	0.016(1)	0.096(5)
C35	0.1013(6)	0.1408(5)	–0.181(1)	0.089(4)
C41	0.3706(4)	0.3534(3)	0.0104(8)	0.051(3)
C42	0.3676(5)	0.3335(4)	–0.1404(8)	0.069(3)
C43	0.3734(7)	0.3876(4)	–0.224(1)	0.095(4)
C44	0.3727(6)	0.4350(4)	–0.121(1)	0.082(4)
C45	0.3772(7)	0.4413(4)	0.144(1)	0.098(4)
B1	0.118(1)	0.1073(6)	0.428(2)	0.107(7)
F11[a]	0.0657(7)	0.1510(5)	0.434(1)	0.133(5)
F12[a]	0.0686(7)	0.0696(5)	0.501(2)	0.148(6)
F13[a]	0.123(2)	0.0933(8)	0.285(1)	0.22(1)
F14[a]	0.1885(6)	0.120(1)	0.485(2)	0.26(1)
F111[b]	0.071(3)	0.075(2)	0.363(7)	0.23(2)[a]
F121[b]	0.155(2)	0.074(1)	0.531(3)	0.152(9)[a]
F131[b]	0.175(2)	0.084(1)	0.345(4)	0.15(1)[a]
F141[b]	0.130(3)	0.157(1)	0.443(3)	0.150(9)[a]
B2	0.6218(7)	0.1141(5)	0.421(1)	0.079(4)
F21[a]	0.6867(8)	0.085(1)	0.446(3)	0.25(1)
F22[a]	0.5597(6)	0.0999(7)	0.513(1)	0.156(6)
F23[a]	0.650(1)	0.1658(5)	0.428(1)	0.141(6)
F24[a]	0.587(1)	0.1042(7)	0.292(1)	0.180(8)
F211[b]	0.678(2)	0.085(1)	0.512(2)	0.089(6)[a]
F221[b]	0.584(2)	0.163(1)	0.451(2)	0.116(7)[a]
F231[b]	0.564(2)	0.078(1)	0.395(4)	0.146(9)[a]
F241[b]	0.667(2)	0.112(1)	0.290(3)	0.135(7)[a]
C/O90[c]	0.46370	0.49783	0.46181	0.34(3)[a]
C/O91[c]	0.37842	0.52619	0.44919	0.33(3)[a]
C/O92[c]	0.32396	0.50757	0.51894	0.31(2)[a]
C/O93[d]	0.25822	0.45983	0.48799	0.36(3)
C/O94[d]	0.65490	0.03020	0.08521	0.28(2)
C/O95[c]	0.71861	–0.01664	0.13966	0.26(2)[a]
C/O96[c]	0.58446	–0.00149	0.10036	0.21(1)[a]

[a] U_{iso}. [b] Occupation factors: (a) $^2/_3$; (b) $^1/_3$; (c) $^1/_2$; (d) $^3/_4$.

(11) Gritzner, G.; Rechberger, P.; Gutman, V. *J. Electroanal. Chem.* **1977**, *75*, 739.
(12) Rechberger, P.; Gritzner, G. *Inorg. Chim. Acta* **1978**, *31*, 125.
(13) Hitchman, M. A. *Transition Met. Chem. (N.Y.)* **1985**, *9*, 1.
(14) Sheldrick, G.M. SHELXTL-Plus. Release 4.0 for Siemens R3 Crystallographic Research Systems. Siemens Analytical X-Ray Instruments, Inc., Madison, WI, 1989.

Table III. Selected Bond Lengths (pm) and Angles (deg) in $Ni(NMTP)_4(BF_4)_2 \cdot 2MeOH$

Ni–S1	228.2(2)	Ni–S2	229.4(2)
Ni–S3	228.6(2)	Ni–S4	228.6(3)
S1–C11	166.7(9)	S–C21	169.1(7)
S3–C31	169.4(7)	S4–C41	169.8(8)
N1–C11	130.9(9)	N1–C14	145.4(11)
N1–C15	145.2(10)	N2–C21	132.0(9)
N2–C24	147.7(10)	N2–C25	145.5(12)
N3–C31	131.3(10)	N3–C34	147.7(11)
N3–C35	145.2(13)	N4–C41	128.2(11)
N4–C44	146.8(12)	N4–C45	146.9(12)
C11–C12	150.3(11)	C12–C13	150.5(12)
C13–C14	151.7(12)	C21–C22	147.1(11)
C22–C23	152.1(10)	C23–C24	149.2(14)
C31–C32	148.4(12)	C32–C33	153.6(11)
C33–C34	147(2)	C41–C42	151.7(11)
C42–C43	151.4(13)	C43–C44	149.1(14)
S1–Ni–S2	119.96(9)	S1–Ni–S3	120.36(9)
S1–Ni–S4	85.12(8)	S2–Ni–S3	85.03(8)
S2–Ni–S4	126.90(9)	S3–Ni–S4	124.02(9)
Ni–S1–C11	109.4(3)	Ni–S2–C21	108.8(3)
Ni–S3–C31	109.1(3)	Ni–S4–C41	109.8(3)
C11–N1–C14	115.7(6)	C11–N1–C15	125.1(7)
C14–N1–C15	119.1(6)	C21–N2–C24	113.5(6)
C21–N2–C25	126.1(6)	C24–N2–C25	120.4(6)
C31–N3–C34	112.6(7)	C31–N3–C35	126.0(7)
C34–N3–C35	121.4(7)	C41–N4–C44	114.3(7)
C41–N4–C45	125.8(7)	C44–N4–C45	119.9(7)
S1–C11–N1	124.4(6)	S1–C11–C12	127.3(6)
N1–C11–C12	108.2(7)	C11–C12–C13	106.1(7)
C12–C13–C14	106.0(7)	N1–C14–C13	103.8(7)
S2–C21–N2	122.7(6)	S2–C21–C22	126.7(5)
N2–C21–C22	110.5(6)	C21–C22–C23	104.6(7)
C22–C23–C24	107.2(7)	N2–C24–C23	103.5(6)
S3–C31–N3	122.3(6)	S3–C31–C32	126.8(5)
N3–C31–C32	110.9(6)	C31–C32–C33	104.1(7)
C32–C33–C34	106.5(9)	N3–C34–C33	105.4(7)
S4–C41–N4	123.9(6)	S4–C41–C42	125.6(6)
N4–C41–C42	110.5(7)	C41–C42–C43	103.6(7)
C42–C43–C44	107.1(8)	N4–C44–C43	104.3(8)

In the Ni^{2+} compound, the cation has no crystallographic symmetry, but shows the pseudosymmetry $\bar{4}2m$ (D_{2d}). In this structure the H atomic positioins were kept "riding" on the C atoms with idealized geometry (C–H 96 pm), and a common isotropic temperature factor was refined, while for the heavier atoms anisotropic temperature factors were used. The two independent BF_4 anions both proved to be positionally disordered. In a disorder model the occupation ratio was 2:1 for the two alternative orientations. Only for the F atoms with the higher occupation number (F^a in Table I) could anisotropic temperature factors be refined. At this stage, the residuals dropped to about R = 13% and R_w = 12%, only. In a difference Fourier map, a ribbonlike region of diffuse electron density remained near the center at 0, $^1/_2$, $^1/_2$. As a large solvent molecule like DMP does not sufficiently well reproduce its geometry, we have assumed strongly disordered methanol molecules which may have formed by reaction of DMP with H_2O. The best results were obtained with a disorder model based on seven atomic positions each half-occupied C and O atoms (Table II), respectively, and with a total contents of two molecules of MeOH per formula unit. Now R and R_w values of 0.083 and 0.086, respectively, resulted as well as rather small standard deviations for the atoms of the $Ni(NMTP)^{2+}$ cation. The atomic parameters are shown in Table II, with the geometrical data given in Table III.

The structure of the Zn^{2+} analogue was solved in a similar way. Here, the cation and the two BF_4 anions have 2 (C_2) symmetry. Disorder is observed only in the solvent part of the structure, which is a DMP molecule in this case. It is also situated on a 2-fold axis, but the methoxy groups show two alternative orientations, described by a 1:1 split atom model. The H atoms were all kept riding on calculated positions, and isotropic temperature factors were refined groupwise. For all other atoms anisotropic temperature factors could be used. The final residuals dropped to R (R_w) = 0.057 (0.047). The resulting atomic parameters are listed in Table IV, with the bond lengths and angles given in Table V.

(15) Cromer, D. T.; Waber, J. T. *International Tables for X-ray Crystallography*; Kynoch Press: Birmingham, England, 1974; Vol. IV.

Table IV. Atomic Parameters and Equivalent Isotropic Temperature Factors in $[Zn(NMTP)_4](BF_4)_2 \cdot DMP$ (Hydrogen Atoms Omitted; C31–36 = DMP Solvent Molecule with Disordered Methoxy Groups)

atom	x	y	z	U_{eq}
Zn	0.00	0.08936(3)	0.25	0.0390(2)
S1	0.1038(1)	0.14243(5)	0.4010(1)	0.0467(4)
S2	0.1157(1)	0.03337(5)	0.1916(1)	0.0505(4)
N1	0.0445(3)	0.2275(2)	0.4989(3)	0.056(2)
N2	0.2245(3)	–0.0586(2)	0.2792(3)	0.052(1)
C11	0.0156(4)	0.1877(2)	0.4261(3)	0.045(2)
C12	–0.1040(4)	0.1891(2)	0.3689(4)	0.060(2)
C13	–0.1461(5)	0.2309(3)	0.4323(5)	0.078(2)
C14	–0.0469(5)	0.2624(2)	0.5031(5)	0.070(2)
C15	0.1537(5)	0.2409(3)	0.5699(5)	0.087(3)
C21	0.1725(3)	–0.0145(2)	0.2916(3)	0.043(1)
C22	0.1723(5)	–0.0130(3)	0.4049(4)	0.075(2)
C23	0.2322(5)	–0.0650(3)	0.4585(4)	0.083(2)
C24	0.2700(4)	–0.0944(2)	0.3766(4)	0.069(2)
C25	0.2366(5)	–0.0761(3)	0.1785(4)	0.096(3)
B1	0.50	0.3303(5)	0.25	0.076(3)
F11	0.4099(3)	0.2972(2)	0.2176(3)	0.113(2)
F12	0.4982(4)	0.3632(2)	0.3335(4)	0.127(2)
B2	0.50	0.1693(4)	0.75	0.068(2)
F21	0.4989(5)	0.1346(2)	0.6692(4)	0.147(2)
F22	0.4116(3)	0.1999(2)	0.7208(5)	0.171(3)
C31	0.50	0.1053(4)	0.25	0.135(5)
C32	0.3979(6)	0.1381(3)	0.2271(7)	0.120(4)
O33[a]	0.4907(8)	0.1003(4)	0.1245(7)	0.108(4)
O34[a]	0.5446(6)	0.0525(4)	0.2870(8)	0.090(4)
C35[a]	0.578(1)	0.0746(7)	0.088(1)	0.128(8)
C36[a]	0.464(2)	0.0094(7)	0.260(3)	0.17(1)

[a] Half-occupied disordered positions.

Table V. Selected Bond Lengths [pm] and Angles [°] in $Zn(NMTP)_4(BF_4)_2 \cdot DMP$

Zn–S1	234.1(1)	Zn–S2	235.1(2)
S1–C11	170.0(5)	S2–C21	169.8(4)
N1–C11	130.1(6)	N1–C14	148.0(8)
N1–C15	144.7(8)	N2–C21	129.1(6)
N2–C24	147.7(6)	N2–C25	145.7(7)
C11–C12	148.9(7)	C12–C13	152.4(8)
C13–C14	150.6(9)	C21–C22	150.0(7)
C22–C23	149.7(8)	C23–C24	151.3(8)
F11–B1	135.9(8)	F12–B1	135.9(8)
F21–B2	134.3(8)	F22–B2	130.8(8)
S1–Zn–S2	109.25(4)	S1–Zn–S1′	115.27(5)
S1–Zn–S2′	105.82(4)	S2–Zn–S1′	105.82(4)
S2–Zn–S2′	111.54(5)	S1′–Zn–S2′	109.25(4)
Zn–S1–C11	105.7(2)	Zn–S2–C21	106.1(2)
C11–N1–C14	113.7(4)	C11–N1–C15	126.8(5)
C14–N1–C15	119.4(4)	C21–N2–C24	114.9(4)
C21–N2–C25	125.6(4)	C24–N2–C25	119.5(4)
S1–C11–N1	124.0(4)	S1–C11–C12	126.3(3)
N1–C11–C12	109.8(4)	C11–C12–C13	105.3(4)
C12–C13–C14	104.8(5)	N1–C14–C13	104.0(4)
S2–C21–N2	123.1(3)	S2–C21–C22	127.2(4)
N2–C21–C22	109.7(4)	C21–C22–C23	105.3(5)
C22–C23–C24	107.0(4)	N2–C24–C23	103.1(4)

Results and Discussion

Crystal Structures. Figures 1 and 2 show the geometries of the zinc and nickel complexes, respectively. The ZnS_4 entity of C_2 symmetry is slightly distorted from the ideal tetrahedral geometry, with S–Zn–S angles deviating between –3.5° and +6° from the tetrahedral angle and Zn–S bond lengths of 234.5 ± 0.5 pm. The nickel complex on the other hand shows a very distinct tetragonal elongation of the tetrahedron as the dominating distortion component, with two pairs of ligands moving towards each other, as illustrated in Figure 3. The latter complex thus approximates D_{2d} symmetry with the trans SNiS angles along the pseudo-S_4 axis decreasing from the tetrahedral angle by almost 25°. This is the largest distortion of a tetrahedral Ni^{2+} complex observed so far. The real symmetry is lower, however. The four

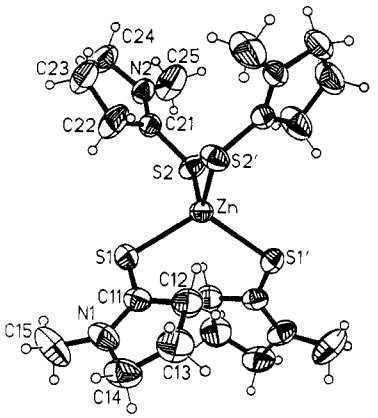

Figure 1. XP[14] drawing of the molecular geometry of the $[Zn(NMTP)_4]^{2+}$ cation (ellipsoids of thermal motion at the 50% probability level).

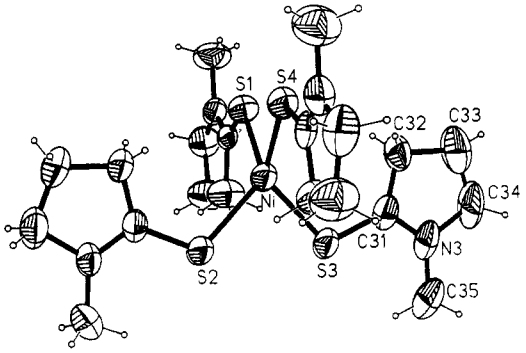

Figure 2. XP[14] drawing of the molecular geometry of the $[Ni(NMTP)_4]^{2+}$ cation (ellipsoids of thermal motion at the 50% probability level).

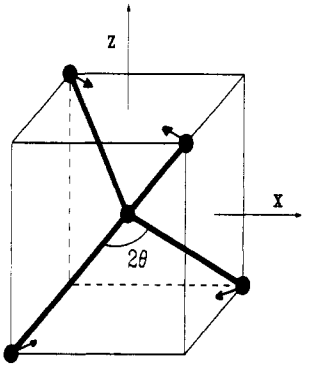

Figure 3. Dominant distortion undergone by the $Ni(NMPT)_4^{2+}$ complex (D_{2d}, elongation).

remaining angles vary between 120 and 127°, indicating that the planes defined by the Ni–S bonds enclosing the angle 2θ are not precisely perpendicular. The nickel–sulfur bond length is practically identical with those found for other four-coordinated nickel–sulfur complexes.[8,9]

The ligands of the $Ni(NMTP)^{2+}$ cation are pairwise coplanar. The maximal deviation from the best plane is 13(2) pm for atoms S2 and S3 and 5(2) pm for S1 and S4. The two pairs of planes are oriented perpendicular to each other with a canting angle of 89.5(2)°. In contrast, the ligands in the zinc complex have a propeller-like arrangement. The structure of the ligand molecules is similar in both complexes, however, though their steric arrangement is different. The distance between the nearest sulfur atoms in the nickel complex is rather short [S1–S4 = 308.9(3) pm; S2–S3 = 309.5(3) pm] compared with the sum of the van der Waals radii (360 pm[16]). A measure of the participation of the two resonance forms of the ligand molecule (see illustration above) is the C*x*1–S*x* and C*x*1–N*x* bond lengths (*x* = 1–4 for the nickel and *x* = 1, 2 for the zinc complex). The C*x*1–N*x* spacings [128–132 pm] are much shorter than the N*x*–C*x*4 and N*x*–C*x*5 bonds [145–148 pm], indicating an appreciable contribution of the resonance form II to the ground-state wave function.

Electronic Spectra. The low-temperature reflectance spectrum of $[Co(NMTP)_4](BF_4)_2$ is shown in Figure 4, together with the spectrum of the analogous zinc complex, which indicates the likely positions of peaks due to vibrational overtones. The local geometries of the MS_4 entities in complexes $[M(NMTP)_4](FB_4)_2$ are expected to be very similar for $M = Zn^{2+}$ and Co^{2+}, because the two ions have nearly identical radii and Jahn–Teller stable nondegenerate groundstates. Indeed the spectrum of the cobalt complex suggests a nearly regular tetrahedral geometry similar to that of the zinc complex. The two broad bands centered at $\simeq$7200 and $\simeq$15 500 cm^{-1} may be assigned to the parity-allowed transitions from the $^4A_2$ ground state to the two $^4T_1$ excited states. Although the presence of infrared overtones makes the identifications of individual peak maxima difficult, it is apparent that the lower energy band in particular is split considerably, perhaps by as much as 3000 cm^{-1}. Such a splitting cannot be explained solely by spin–orbit coupling, which should not exceed 2000 cm^{-1}. Presumably an additional contribution due to low-symmetry ligand field components is also present. The CAMMAG[17] calculation suggests a value of $\approx$500 cm^{-1} for the latter, assuming the structure to be very similar to that of the zinc complex. The shoulder around 13 500 cm^{-1} should be due to spin-forbidden transitions to a $_a^2E$ and a $_a^2T_1$, and the weak bands at $\simeq$19 500 cm^{-1} and $\simeq$22 500 cm^{-1} should correspond to the transitions to $_b^2T_2$, $_b^2T_1$, $_b^2E$ and $_c^2T_1$, $_d^2T_1$, $_c^2T_2$, respectively. The $^4A_2 \rightarrow {}^4T_2$ transition, which is expected to lie at about 4000 cm^{-1}, may occur below the cutoff region of the spectrophotometer; this transition should have a low intensity, as it is parity forbidden. The best-fit parameters are Δ = 4200 cm^{-1} and B = 675 cm^{-1}, corresponding to a nephelauxetic ratio of $\beta \simeq 0.69_5$ (B_0 = 970 cm^{-1}). This value is distinctly lower than that for oxygen as a ligand ($\beta \simeq 0.81$), although the Δ value is comparable ($\simeq$4100 cm^{-1}).

The powder reflection spectra of $[Zn(NMTP)_4](BF_4)_2$ containing about 30 mol % nickel(II) as dopant, measured at 293 and 5 K, is given in Figure 5. The spectrum of the (010) crystal face, with the electric vector along the two extinction directions, is given in the diagram insert. The band positions were observed to be virtually identical to those of the pure nickel(II) complex. Intense bands appear at $\simeq$5500 and $\simeq$15 200 cm^{-1} with weaker peaks at 8700 and $\simeq$12 500 cm^{-1} and a shoulder at $\simeq$17 800 cm^{-1}. The shoulder at $\approx$6000 cm^{-1} corresponds to a peak, which is also present in the spectrum of the analogous Zn^{2+} complex, and may therefore be an infrared overtone or a combination band. Well-resolved bands centered at $\simeq$14 500 and 15 500 cm^{-1} were observed in the single-crystal spectrum, the lower energy peak being significantly polarized. These peak positions are in reasonable agreement with those reported by Rechberger and Gritzner[12] for $[Ni(NMTP)_4](ClO_4)_2$ dissolved in the ligand as solvent, with the proviso that the transitions observed in the reflectance spectrum at $\simeq$12 500 and $\simeq$17 800 cm^{-1} are not seen in the solution or crystal spectra. The similarity between the spectra of the doped and the pure Ni^{2+} complexes suggests that the geometry of the $Ni(NMTP)^{2+}$ cation in the zinc host lattice closely matches that of the pure compound.

The observed transition energies are summarized in Table VI, together with assignments using symmetry labels appropriate to

(16) Weiss, A.; Witte, H. *Crystal Structure and Chemical Bonding*; Verlag Chemie: Weinheim, Germany, 1983.

(17) Cruse, D. A.; Davies, J. E.; Gerloch, M.; Harding, J. H.; Mackey, D. J.; McMeecking, R. F. CAMMAG, a Fortran computer package. University Chemical Laboratory, Cambridge, England, 1979.

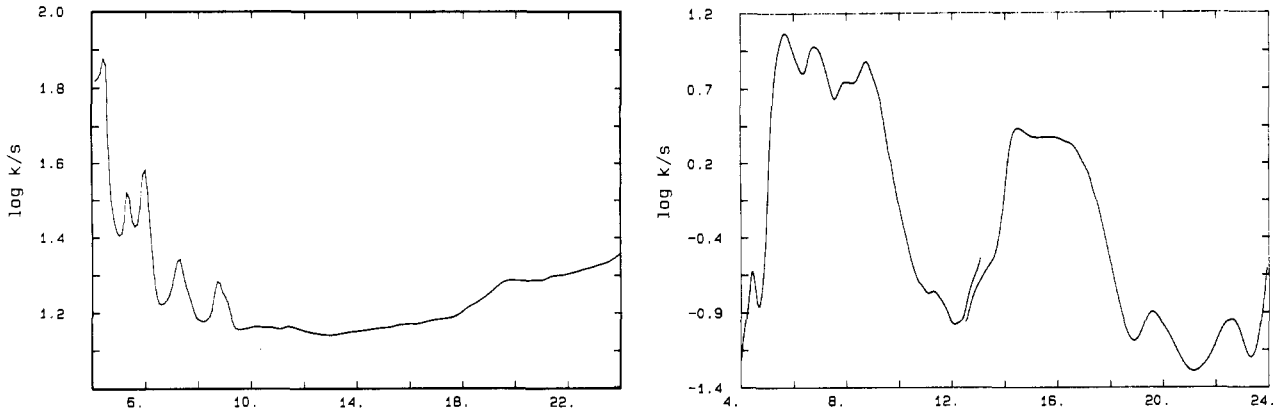

Figure 4. Reflectance spectra of $[Co(NMTP)_4](BF_4)_2$ at 5 K (right) and $[Zn(NMTP)_4](BF_4)_2$ at 295 K (left), with energies given in 10^3 cm^{-1}.

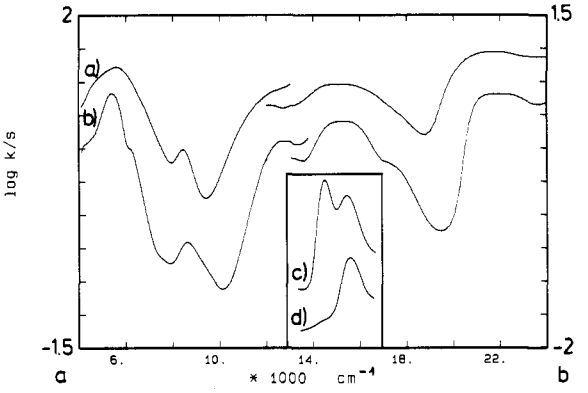

Figure 5. Reflectance spectra of Ni^{2+}-doped $[Zn(NMTP)_4](BF_4)_2$ (≈30 mol %) at 295 K (a) and 5 K (b). Spectra of the (010) crystal face of the Ni^{2+} doped complex at 15 K, with the electric vector of polarized light along the two extinction directions are shown as an insert, curves c and d. The orientation of the electric vector with respect to the pseudo-S_4 axis of the $Ni(NMTP)_2^{2+}$ cation is unknown.

the D_{2d} point group, but specifying the tetrahedral parent terms also. In an elongated D_{2d} geometry the transitions ${}_a{}^3A_2 \rightarrow {}^3B_2$ and ${}_b{}^3A_2$ are orbitally forbidden, but may be present with weak intensiity due to the lower symmetry of the NiS_4 polyhedron. In Table 6 also the transition energies calculated using the CAMMAG program[17] are given, both using the geometry of the NiS_4 polyhedron, as revealed by the structure analysis (I), and an idealized D_{2d} geometry (II). The best fit parameters are discussed in the next section.

The comparison of the calculations with the true and an idealized D_{2d} geometry reveals that the lower-symmetry component is very small, inducing energy shifts due to term splittings of always less than 300 cm^{-1}. The two weak features at 8700 and 17 800 cm^{-1} may therefore be due to an infrared ligand overtone and a series of spin-forbidden bands, respectively (Table VI), rather than to the symmetry-forbidden ${}_a{}^3A_2 \rightarrow {}^3B_2, {}_b{}^3A_2$ transitions (Figures 4 (left) and 5b). Indeed it is not possible to find a parameter set which matches their energy positions with the calculated ${}_a{}^3A_2 \rightarrow {}^3B_2$ and ${}_b{}^3A_2$ transitions.

The pair of peaks at ≃14 500 and ≃15 350 cm^{-1} is tentatively assigned to transitions to the split components of the ${}_c{}^3E$ (${}_b{}^3T_1$) term in Table VI. However, the observed splitting is considerably larger than that calculated using the AOM (see following section), suggesting that it is caused by something other than the fact that the molecular geometry deviates slightly from D_{2d} symmetry. Calculations were also carried out including spin–orbit coupling, but this only increased the energy separation between the highest and lowest energy levels, originating from ${}_c{}^3E$, to about 500 cm^{-1}. An alternative assignment for the 14 500 cm^{-1} band is that it is due to the ${}_a{}^3A_2 \rightarrow {}_a{}^1A_1$ transition, though the intensity is very high for a spin-forbidden band. However, a spin-forbidden transition may gain intensity if it is almost coincident with a spin-allowed band. Perhaps the best known example is the ${}^3A_{2g}$–$({}^3T_{2g}, {}^1E_g)$ transitions of the $Ni(H_2O)_6^{2+}$ ion, where a splitting of ≃1200 cm^{-1} is observed.[18] A small increase of the C/B ratio could indeed generate a situation of this kind. A further alternative is that the splitting is due to a lowering in symmetry of the ${}_c{}^3E$ (${}_b{}^3T_1$) excitated state by vibronic coupling. Splittings of ≃1500 cm^{-1} in the ${}^2B_1$–${}^2E$ transition of the VO_4^{4-} complex (elongated D_{2d} geometry), doped into various host lattices of the $ZrSiO_4$ type, have been ascribed to this cause.[19] However, band splittings due to "dynamic" Jahn–Teller effects in the excited electronic state usually alter significantly as a function of temperature,[20] and in the present case the splitting at 298 K was observed to be essentially identical to that 12 K, which tends to argue against this mechanism. The fact that the splitting is observed in both solution and single-crystal spectra suggests that the cause is an inherent property of the complex, rather than a crystal packing effect. The origin of the strong polarization of the peak centered at 14 500 cm^{-1} in the crystal spectrum is also not clear.

Metal–Ligand Bonding Parameters. To investigate the metal–ligand bonding in the complexes the transition energies were calculated using the computer program CAMMAG developed by Gerloch and co-workers.[17] This program parametrizes the metal–ligand interactions in terms of AOM σ- and π-bonding parameters e_σ and e_π,[21] with the geometry being specified using the stereochemistry indicated by the crystal structure of each complex.

The spectrum of the $[Co(NMTP)_4]^{2+}$ complex suggests a ligand field splitting parameter $\Delta \simeq 4200$ cm^{-1} and a Racah parameter $B \simeq 675$ cm^{-1} ($\beta = 0.69_5$). The NMTP ligand thus lies considerably higher than chloride in the spectrochemical series and also has a somewhat greater nephelauxetic effect ($CoCl_4^{2-}$: $\Delta \simeq 3150$ cm^{-1}, $\beta \simeq 0.73$).[18] Because the complex has an evidently nearly undistorted tetrahedral geometry, it is impossible to determine the metal–ligand σ- and π-bonding parameters independently, and effects due to configuration interaction with the metal 4s orbital will be negligible.

The transition energies of the NiS_4 polyhedron with approximate D_{2d} symmetry are rather sensitive to the ratio between the σ- and π-bonding parameters, and to the anisotropy of the π-bonding about the metal–ligand bond axis. The anisotropic π-antibonding energy contributions were evaluated using the parameters e_π^x and e_π^y, the former representing the π-interaction in the plane of the ligand and the latter representing that out of this plane.[21] In addition, it has been found that for complexes

(18) Lever, A. B. P. *Inorganic Electronic Spectroscopy*, 2nd ed.; Elsevier: Amsterdam, 1984; pp 507, 740.
(19) DiGregono, S.; Greenblatt, M.; Pifer, J. H.; Sturge, M. D. *J. Chem. Phys.* **1982**, *76*, 2931.
(20) Bersuker, I. B. *The Jahn-Teller Effect and Vibronic Interactions in Modern Chemistry*; Plenum Press: New York, 1984; Chapter 4.
(21) Schäffer, C. E. *Struct. Bonding (Berlin)* **1973**, *14*, 69. Larsen, E.; La Mar, G.N. *J. Chem. Educ.* **1974**, *51*, 633. Smith, D. W. *Struct. Bonding (Berlin)* **1978**, *35*, 87.

Table VI. Observed and Calculated d–d Transitions for Ni^{2+} (d^8) in $Zn(NMTP)_4^{2+}$ [a]

	transition energies, cm^{-1}					
			calculated			
	observed		I		II	
excited state	reflection[b]	solution[c]	triplets	singlets	triplets	singlets
$^3{}_aE\ (^3{}_aT_1)$	*d*		4080, 4140		4090	
$^3{}_bE\ (^3T_2)$	5500		5180, 5420		5240	
$^1{}_aB_2\ (^1{}_aT_2)$				10110		10230
$^1{}_aB_1\ (^1{}_aE)$				10180		10285
$^3B_2\ (^3T_2)$	(8700)[e]	(8300)[e]	10410		10330	
$^3B_1\ (^3A_2)$	~12300		11720		11710	
$^1{}_aE\ (^1{}_aT_2)$				13260, 13320		13630
$^1{}_aA_1\ (^1{}_aE)$				14350		14275
$^3{}_cE\ (^3{}_bT_1)$	15200	14500,[f] 15350[f]	15560, 15700		15550	
$^1{}_bE\ (^1{}_bT_2)$	~17800			17150, 17310		18530
$^1{}_cE\ (^1T_1)$				18440, 18710		19325
$^3{}_bA_2\ (^3{}_bT_1)$	*d*		19550		19550	

[a] For the best fit AOM parameters used, see eq 1. Symmetry labels are those of the D_{2d} point group [$^3{}_aA_2\ (^3{}_aT_1)$ ground term]; T_d parent terms are given in brackets. Calculation I is based on the observed molecular geometry; II is based on an idealized D_{2d} symmetry. [b] Reflectance spectrum of $[Zn_{0.7}Ni_{0.3}(NMTP)_4](BF_4)_2$. [c] Spectrum reported[12] for $[Ni(NMTP)_4](ClO_4)_2$ in a NMTP solution. [d] Region obscured by infrared overtones or charge-transfer absorption. [e] Possibly due to an infrared overtone. [f] Bands at 14 500 and 15 500 cm^{-1} were observed in the spectrum of a crystal of $[Zn_{0.7}Ni_{0.3}(NMTP)_4](BF_4)_2$ as well.

in which the symmetry is lower than cubic the metal d_{z^2} orbital is depressed in energy compared with the predictions of simple bonding schemes. The AOM relates the depression to configuration interaction between the metal 4s and $3d_{z^2}$ orbitals,[22] and in the MO-based treatment developed by Smith[23] a parameter e_{ds} is conventionally used to describe the effect. Recently Gerloch and co-workers demonstrated, however, that fundamental objections exist against extending the d-basis set by including the s-orbital in a ligand field based AOM treatment.[24,25] They proposed in a novel AOM version to account for the $d_{z^2}s$ interaction by introducing a parameter e_σ(void), which becomes directly apparent in a square-planar coordination as a negative energy. Though the authors are aware of the inconsistencies in using e_{ds} they stick to a parametrization including e_{ds} for two reasons. Without stressing the absolute numerical magnitudes of this parameter too much, the trend of the e_{ds} values when comparing analogous complexes with different coordination numbers and geometries gives some qualitative insight into the energy effect related to the nd_{z^2} depression by the interaction with the $(n+1)$s orbital. It is indeed apparent that a close correlation exists between the magnitude of e_{ds} and the s contribution to the d_{z^2} ground state, as revealed by the hyperfine structure in the EPR spectra of tetragonally compressed CuL_6 octahedra.[26] Second, most of the literature data is parametrized in terms of AOM parameter sets including e_{ds} and allows a direct comparison with our data.

The energy levels of the complex were calculated for a wide range of AOM parameters, and the optimum fit between the calculated and observed transition energies was obtained using the set

$$e_\sigma = 5000\ cm^{-1};\ e_\pi{}^x = 1000\ cm^{-1};\ e_\pi{}^y = 1500\ cm^{-1};$$
$$e_{ds} = 1500\ cm^{-1};\ B = 700\ cm^{-1}\ (\beta = 0.67);\ C/B = 4.0 \quad (1)$$

The calculated transition energies, with spin–orbit coupling set to zero, are given in Table VI.

Using the relationship $\Delta = {}^4/_9(3e_\sigma - 2e_\pi{}^x - 2e_\pi{}^y)$ the above parameters correspond to a ligand field splitting of 4450 cm^{-1} for a complex $[Ni(NMTP)_4]^{2+}$ with a regular tetrahedral geometry, again considerably greater than that reported[27] for the corresponding chloride complex (Δ = 3700 cm^{-1}). The reduction of ≈33% in the interelectron repulsion parameter B compared with the free ion value confirms that the NMTP ligand has a rather strong nephelauxetic effect, somewhat greater than that of the chloride ligands in $NiCl_4^{2-}$ (28%).[18] For NiO_4 tetrahedra, Δ and β values of 4200 cm^{-1} and 0.82, respectively, are reported.[4] The bonding properties of the S ligator atom in NMTP are distinctly different from those of thioethers. For example 1,4,7-trithiacyclononane (TTCN) induces a β-value of 0.77 in an octahedral Ni^{2+} complex, indicating a comparatively much more ioinic bond.[28] Also the hypothetical Δ value of TTCN for a tetrahedral coordination ($\Delta \approx {}^1/_2\Delta_0 \simeq$ 6300 cm^{-1}) is considerably higher.

The above bonding parameters suggest that, in agreement with the proposals in [4], the rather large Jahn–Teller distortion observed for the $[Ni(NMTP)_4]^{2+}$ complex compared with $NiCl_4^{2-}$ is indeed associated with a moderately large ligand field splitting parameter and a rather strong nephelauxetic effect for the sulfur-donor ligand. The π-bonding parameters are similar to those observed for a range of nitrogen and oxygen donor ligands toward nickel(II),[29] being about 25% of the e_σ value. The C–S–Ni angle is very close to the tetrahedral angle (Table III), implying sp^3 hybridization of the sulfur orbitals. Apparently the e_π parameters represent interactions with "nonbonding" sulfur lone electron pairs of pseudotetrahedral symmetry, and effects of this type have been documented in other systems also.[30] It is possible that the Ni–S bond vector deviates somewhat from the direction of the orbital on the sulfur. Such "off-axis" bonding seems to influence the bonding parameters in a number of metal(II) complexes.[31] It may also be noted that the contribution of resonance structure II to the wave function of the ligand is expected to affect the

(22) Ceulemans, A.; Beyens, D.; Vanquickenborne, L. G. *Inorg. Chim. Acta* **1982**, *61*, 199. Vanquickenborne, L. G.; Ceulemans, A. *Inorg. Chem.* **1981**, *20*, 796.
(23) Smith, D. W. *Inorg. Chim. Acta* **1977**, *22*, 107.
(24) Gerloch, M.; Harding, J. H.; Wooley, G. *Struct. Bonding (Berlin)* **1981**, *46*, 1.
(25) Deeth, R. J.; Gerloch, M. *Inorg. Chem.* **1984**, 23, 3846 and references therein.
(26) Steffen, G.; Reinen, D.; Stratemeier, H.; Riley, M. J.; Hitchman, M. A.; Matthies, H. E.; Recker, K.; Wallrafen, F.; Niklas, J. R. *Inorg. Chem.* **1990**, *29*, 2123.
(27) Goodgame, M.; Goodgame, D. M. L.; Cotton, F. A. *J. Chem. Soc.* **1961**, *83*, 4161; Schmidtke, H.-H. Private communication.
(28) Reinen, D.; Ozarowski, A.; Jakob, B.; Pebler, J.; Stratemeier, H.; Wieghardt, K.; Tolksdorf, I. *Inorg. Chem.* **1987**, *26*, 4010.
(29) Bencini, A.; Benelli, C.; Gatteschi, D. *Coord. Chem. Rev.* **1984**, *60*, 131.
(30) Deeth, R. J.; Duer, M. J.; Gerloch, M. *Inorg. Chem.* **1987**, *26*, 2573.
(31) Deeth, R. J.; Duer, M. J.; Gerloch, M. *Inorg. Chem.* **1987**, *26*, 2578, 2582.

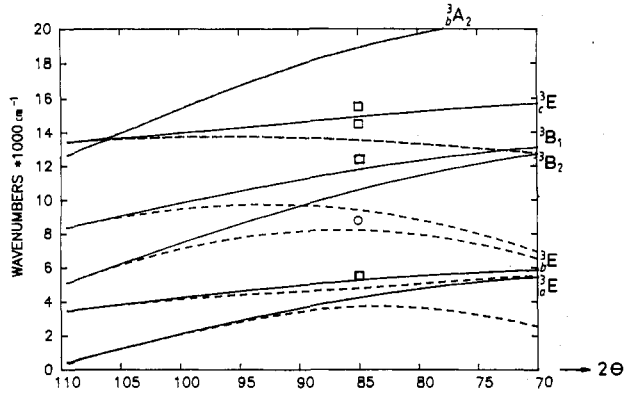

Figure 6. Energy variation of the spin-triplet terms of a distorted tetrahedral nickel(II) complex of idealized D_{2d} symmetry [$_a{}^3A_2$ ($_a{}^3T_1$) ground state], calculated as a function of the 2θ distortion angle, including (full lines; e_{ds} = 1500 cm^{-1}) and neglecting (dashed lines) "d-s mixing". For the used parameters see eq (1). The e_π anisotropy induces a splitting of the tetrahedral parent terms $_a{}^3T_1$, $^3T_2$, $_b{}^3T_1$ even at 2θ = 109.5°. The observed transitions are indicated by squares, those with a doubtful assignment by circles.

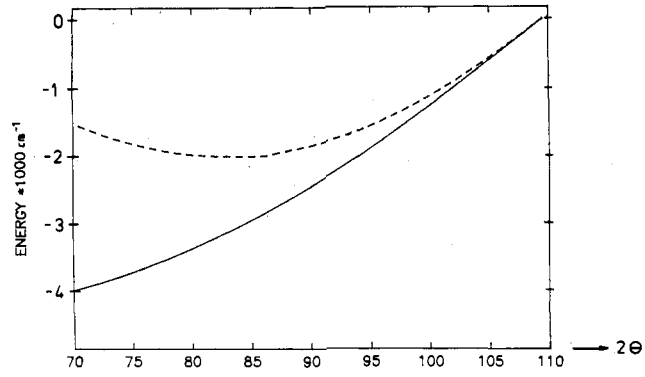

Figure 7. Changes of the $_a{}^3A_2$ ($_a{}^3T_1$) ground state energy of the Ni(NMTP)$^{2+}$ cation as a function of distortion from a regular tetrahedral geometry (parameters as in Figure 6), both including (full line) and neglecting (dashed line) "d-s mixing".

out-of-plane π-interaction, which may be one reason why $e_\pi{}^y$ is larger than $e_\pi{}^x$. However, the rather complex bonding structure of the ligand precludes any simplistic interpretation of the bonding parameters, which should be taken as representing the integral of all of the above effects. Optimum agreement with experiment is obtained if the d_{z^2} orbital is depressed in energy by $\Delta E \simeq 2500$ cm^{-1} compared with the expectation of simple bonding schemes, and this may be related to the distortion angle θ by the expression[23]

$$\Delta E = -4e_{ds}(3\cos^2\theta - 1)^2 \qquad (2)$$

in a D_{2d} complex (Figure 3). For an angular distortion of 25° away from the tetrahedral angle and with e_{ds} = 1500 cm^{-1}, an energy decrease of 2390 cm^{-1} results if the trans ligands approach one another (θ = 42°), but one of only 1770 cm^{-1} results if they move further apart (θ = 67°). The influence which d–s mixing has upon the energy levels of a distorted tetrahedral nickel(II) complex is illustrated in Figure 6, which shows how these vary as a function of the angle 2θ, both including and neglecting e_{ds}. It may be seen that for large angular distortions d–s mixing has a significant effect on most of the energy levels, and agreement with the experimental transition energies becomes poor when this is neglected. Without emphasizing the quantitative aspects of the latter consideration too much (see above), it nevertheless gives some insight into the basic bonding situation. The transition energies observed for [Ni(NMTP)$_4$](BF$_4$)$_2$ and assigned to spin-allowed transitions are also indicated in Figure 6. The comparatively small influence of spin–orbit coupling is not taken into account in these plots.

Using the set of parameters derived from the Ni^{2+} spectra (eq 1 with e_π = 1250 cm^{-1}), one can readily calculate all the vibronic coupling parameters of the Jahn–Teller unstable tetrahedral $_a{}^3T_1$ parent ground state (T $\otimes$ ϵ interaction) on the basis of the formalism, developed in ref 4 (for vanishing spin–orbit coupling):

$$\rho_m = R[2\theta_t - 2\theta] = 0.98\ \text{Å} \qquad V_e{}^{eff} = 2865\ \text{cm}^{-1}\ \text{Å}^{-1}$$
$$L_e{}^{eff} = 890\ \text{cm}^{-1}\ \text{Å}^{-2} \qquad K_e = 2035\ \text{cm}^{-1}\ \text{Å}^{-2}$$
$$E_m = -1405\ \text{cm}^{-1} \qquad \delta E = 3575\ \text{cm}^{-1} \qquad (3)$$

Here ρ_m is the distortion parameter, which acts along the D_{2d} nuclear displacement path of the Jahn–Teller active component of the ϵ mode (see Figure 3). V_e and L_e are the first- and second-order vibronic coupling constants. The notation "eff" means that the intermixing between the two $^3T_1$ states has been taken into account (the $_a{}^3T_1$ ground state wave function contains $\simeq$10.5% excited state contribution, compared to $\simeq$12.5% for $NiCr_2O_4$ and $NiCl_4{}^{2-}$). K_e is the harmonic force constant of the ϵ mode, E_m the vibronic ground-state stabilization energy and δE the $_a{}^3T_1$ ground-state splitting, which is well in accord with the CAMMAG calculation with e_{ds} = 0 (Figure 6). The electronic contribution to E_m is larger than the quoted E_m value in eq 3 by $-1/_2K_e\rho_m{}^2$ and amounts to −2380 cm^{-1}. The variation of the ground-state energy as a function of the angle 2θ should also provide an estimate of the vibronic coupling coefficients for the [Ni(NMTP)$_4$]$^{2+}$ complex. This is shown in Figure 7, both including and neglecting a d_{z^2} stabilization effect (eq 2). If this is ignored, the rate at which the ground-state energy falls as a function of the distortion angle is highly nonlinear and even changes sign at about the angle observed experimentally for this complex (85°). However, when the d_{z^2} depression is included, the energy decreases approximately linearly in the range 90° < 2θ < 109.5°, and the slope of the plot indicates a coupling coefficient $V_e{}^{eff} \simeq 130$ cm^{-1}/deg or $\simeq$3250 cm^{-1}/Å for the observed NiS bond length of 2.29 Å. The linear coupling constant is larger by 13% compared to that in (3), while the second order constant seems to be rather small (Figure 7). The following ground-state properties result:

$$V_e{}^{eff} = 3250\ \text{cm}^{-1}\ \text{Å}^{-1} \quad K_e = 3315\ \text{cm}^{-1}\ \text{Å}^{-2} \quad L_e{}^{eff} \simeq 0$$
$$E_m = -1595\ \text{cm}^{-1} \qquad \delta E = 4780\ \text{cm}^{-1} \qquad (4)$$

The electronic ground-state stabilization is 3185 cm^{-1} in this case, indicating that energy contributions due to $3d_{z^2}$–4s interactions seem to support the driving force of the Jahn–Teller distortion in a significant manner. An effective force constant of $K_e{}^{eff} \simeq$ 3000 cm^{-1} Å^{-2} = 0.06 mdyn Å^{-1} (eqs 3 and 4) implies that the Jahn–Teller active vibration is rather "soft". Here $K_e{}^{eff} = K_e + L_e$, where L_e represents the second-order Jahn–Teller contribution, which adds to the cubic K_e value, due to vibronic coupling.[4] For the strongly compressed $CuCl_4{}^{2-}$ complex a value of 3700 cm^{-1} Å^{-2} is reported,[33] and about the same value should be valid for tetrahedral $NiCl_4{}^{2-}$. Thus one additional reason that a Jahn–Teller distortion is observed in case of Ni(NMTP)$_4{}^{2+}$ and not for $NiCl_4{}^{2-}$, is apparently the smaller ϵ-mode force constant of the former complex, because the vibronic coupling constants don't differ too much. A similar argument holds for Ni^{2+} in $ZnCr_2O_4$, where the force constant is very high (16 450 cm^{-1} Å^{-2}).[4] It reflects the rigidity of the spinel lattice with interconnected polyhedra and possibly also the strong interligand repulsion in case of the negatively charged oxygen, as compared to the sulfur ligator atoms with practically no charge. One may conclude, that the considerable Jahn–Teller distortion of the Ni(MNTP)$_4{}^{2+}$

(32) Hitchman, M. A.; Bremner, J. B. *Inorg. Chim. Acta* **1978**, *27*, L61. Ford, R. J.; Hitchman, M. A. *Inorg. Chim. Acta* **1979**, *33*, L167. Mackey, D. J.; McMeeking, R. F.; Hitchman, M. A. *J. Chem. Soc., Dalton Trans.* **1979**, 299.

(33) Bacci, M. *Chem. Phys.* **1979**, *40*, 237.

complex is the consequence of a rather high Δ/B value, but it is most probably mainly due to a weak restoring force.

The present results suggest that Jahn–Teller coupling coefficients may usefully be estimated by calculating—with the inclusion of e_{ds}—in which way the ground-state energy alters as a function of a geometry change along a Jahn–Teller active normal coordinate. Calculations of this kind should be particularly valuable in situations such as the present one, where tabulated expressions using angular overlap bonding parameters[4,33,34] cannot be used in a simple manner because of the influence of interelectron repulsion.

Conclusions

The substantial distortion of the $[Ni(NMTP)_4]^{2+}$ complex away from the nearly regular tetrahedral geometry observed for the corresponding zinc complex follows the predictions of the Jahn–Teller theorem. In agreement with previous predictions[4] of the properties of ligands likely to produce significant Jahn–Teller distortions in tetrahedral nickel(II) complexes, the analysis of the electronic spectrum suggests that the NMTP ligand is a moderately strong σ- and π-donor and has a rather large nephelauxetic effect.

The stabilization of the d_{z^2} orbital, conventionally interpreted in terms of configuration interaction between the metal 4s and $3d_{z^2}$ orbitals,[23-25] apparently has a significant effect upon the energy levels of the distorted nickel(II) complex. The presented calculations produce an estimate of the coupling coefficient of the Jahn–Teller active vibration which is consistent with the structural distortion observed for the $[Ni(NMTP)_4]^{2+}$ complex, suggesting that the type of analysis should provide a useful way of investigating Jahn–Teller interactions in other systems.

Acknowledgment. Dr. M. Gerloch of the Chemistry Department of the University of Cambridge, United Kingdom, is thanked for making available a copy of the computer program CAMMAG and for helpful suggestions. Financial support from the Australian Research Commission, the Alexander von Humboldt Stiftung (to M.A.H.), the Deutsche Forschungsgemeinschaft (to A.W.) and the Fonds der chemischen Industrie is gratefully acknowledged. The authors owe thanks to Dr. M. Atanasov from the Bulgarian Academy of Sciences, Sofia, for valuable discussions and Miss. S. Wocadlo for technical assistance.

Supplementary Material Available: Additional material from the crystal structure investigations is obtainable from Fachinformationszentrum Karlsruhe, Gesellschaft für wissenschaftlich-technische Information mbH, D-7514 Eggenstein-Leopoldshafen 2, Germany, by giving Deposit No. CSD-56831, the authors, and the journal reference.

(34) Reinen, D.; Atanasov, M. *Magn. Reson. Rev.* **1991**, *15*, 167.